J|A|C|S
ARTICLES
Published on Web 05/10/2002

Detailed Unfolding and Folding of Gaseous Ubiquitin Ions Characterized by Electron Capture Dissociation

Kathrin Breuker,† HanBin Oh, David M. Horn,‡ Blas A. Cerda,§ and Fred W. McLafferty*

Contribution from the Department of Chemistry and Chemical Biology, Baker Laboratory, Cornell University, Ithaca, New York 14853-1301

Received October 1, 2001

Abstract: The unfolding enthalpy of the native state of ubiquitin in solution is 5 to 8 times that of its gaseous ions, as determined by electron capture dissociation (ECD) mass spectrometry. Although two-state folding occurs in solution, the three-state gaseous process proposed for this by Clemmer and co-workers based on ion mobility data is supported in general by ECD mass spectra, including relative product yields, distinct ΔH(unfolding) values between states, site-specific melting temperatures, and folding kinetics indicating a cooperative process. ECD also confirms that the 13+ ions represent separate conformers, possibly with side-chain solvated α-helical structures. However, the ECD data on the noncovalent bonding in the 5+ to 13+ ions, determined overall in 69 of the 75 interresidue sites, shows that thermal unfolding proceeds via a diversity of intermediates whose conformational characteristics also depend on charge site locations. As occurs with increased acidity in solution, adding 6 protons to the 5+ ions completely destroys their tertiary noncovalent bonding. However, solvation of the newly protonated sites to the backbone instead increases the stability of the secondary structure (possibly an α-helix) of these gaseous ions, while in solution these new sites aid denaturation by solvation in the aqueous medium. Extensive ion equilibration can lead to even more compact and diverse conformers. The three-state unfolding of gaseous ubiquitin appears to involve ensembles of individual chain conformations in a "folding funnel" of parallel reaction paths. This also provides a further caution for characterizing solution conformers from their gas-phase behavior.

Introduction

The biological function of a protein can directly depend on its noncovalent bonding to another species and/or to itself. For a deeper understanding of the molecular determinants of this bonding, a number of methods have studied the effect of removing the aqueous phase.[1−3] Methods that measure the ion collision cross section[1] or H/D exchange[2] of a gaseous protein conformer yield only a single parameter, and thus provide no structural details, while data from collisionally activated dissociation (CAD) mass spectrometry (MS) of deuterated conformer ions can be compromised by accompanying H/D scrambling.[2d,f,g] Recently it has been shown[3] that electron capture dissociation (ECD)[4] of gaseous cytochrome *c* ions provides site-specific information on both their thermal unfolding and their pulsed IR laser-induced unfolding and refolding at 60 of the 103 interresidue locations. Here ECD provides noncovalent bonding data at 69 of the 75 interresidue locations of bovine ubiquitin gaseous ions (5+ to 13+) to determine thermal (25−175 °C) unfolding enthalpies, conformational melting temperatures, and kinetics of pulsed laser unfolding and refolding.

The cytochrome *c* ECD study[3] indicated a multiplicity of folding intermediates in addition to the seven stable conformers found by H/D exchange,[2d] in apparent contrast to the classical view of protein folding that proceeds through obligatory intermediates with partial native structures.[5a−c] The "new" view proposes a "folding funnel" in which diverse noncovalent

* Corresponding author. E-mail: fredwmcl@aol.com.
† Present address: Chemistry Department, University of Innsbruck, Austria.
‡ Present address: Genomics Institute of the Novartis Research Foundation, San Diego, CA 92121.
§ Present address: Perkin Elmer Life Sciences, Norton, OH 44203.

(1) (a) Valentine, S. J.; Counterman, A. E.; Clemmer, D. E. *J. Am. Soc. Mass Spectrom.* **1997**, *8*, 954−961. (b) Hoagland, C. S.; Valentine, S. J.; Sporleder, C. R.; Reilly, J. P.; Clemmer, D. E. *Anal. Chem.* **1998**, *70*, 2236−2242. (c) Li, J.; Taraska, J. A.; Counterman, A. E.; Clemmer, D. E. *Int. J. Mass Spectrom.* **1999**, *185/186/187*, 37−47. (d) Jarrold, M. F. *Acc. Chem. Res.* **1999**, *32*, 360−367. (e) Hoaglund-Hyzer, C. S.; Counterman, A. E.; Clemmer, D. E. *Chem. Rev.* **1999**, *99*, 3037−3079. (f) Jarrold, M. F. *Annu. Rev. Phys. Chem.* **2000**, *51*, 179. (g) Purves, R. W.; Barnett, D. A.; Ells, B.; Guevremont, R. *J. Am. Soc. Mass Spectrom.* **2000**, *11*, 738−745. (h) Purves, R. W.; Barnett, D. A.; Ells, B.; Guevremont, R. *J. Am. Soc. Mass Spectrom.* **2001**, *12*, 894−901.

(2) (a) Suckau, D.; Shi, Y.; Beu, S. C.; Senko, M. W.; Quinn, J. P.; Wampler, F. M., III; McLafferty, F. W. *Proc. Natl. Acad. Sci.* **1993**, *90*, 790−793. (b) Zhang, X.; Cassady, C. J. *J. Am. Soc. Mass Spectrom.* **1996**, *7*, 1211−1218. (c) Cassady, C. J.; Carr, S. R. *J. Mass Spectrom.* **1996**, *31*, 247−254. (d) McLafferty, F. W.; Guan, Z.; Haupts, U.; Wood, T. D.; Kelleher, N. L. *J. Am. Chem. Soc.* **1998,** *120*, 4732−4740. (e) Freitas, M. A.; Hendrickson, C. L.; Emmett, M. R.; Marshall, A. G. *Int. J. Mass Spectrom.* **1999**, *185/186/187*, 565−575. (f) Buijs, J.; Hagman, C.; Hakansson, K.; Richter, J. H.; Hakansson, P.; Oscarsson, S. *J. Am. Soc. Mass Spectrom.* **2000**, *12*, 410−419. (g) Reed, D. R.; Kass, S. R. *J. Am. Soc. Mass Spectrom.* **2001**, *12*, 1163−1168.

(3) Horn, D. M.; Breuker, K.; Frank, A. J.; McLafferty, F. W. *J. Am. Chem. Soc.* **2001**, *123*, 9792−9799.

(4) (a) Zubarev, R. A.; Kelleher, N. L.; McLafferty, F. W. *J. Am. Chem. Soc.* **1998**, *120*, 3265−3266. (b) Zubarev, R. A.; Kruger, N. A.; Fridriksson, E. K.; Lewis, M. A.; Horn, D. M.; Carpenter, B. K.; McLafferty, F. W. *J. Am. Chem. Soc.* **1999**, *121*, 2857−2862. (c) Zubarev, R. A.; Horn, D. M.; Fridriksson, E. K.; Kelleher, N. L.; Kruger, N. A.; Lewis, M. A.; Carpenter, B. K.; McLafferty, F. W. *Anal. Chem.* **2000**, *72*, 563−573. (d) Horn, D. M.; Ge, Y.; McLaferty, F. W. *Anal. Chem.* **2000**, *72*, 4778−4784. (e) Kruger, N. A.; Zubarev, R. A.; Carpenter, B. K.; Kelleher, N. L.; Horn, D. M.; McLafferty, F. W. *Int. J. Mass Spectrom.* **1999**, *182/183*, 1−5.

associations lead to ensembles of individual chain conformations that can fold in parallel reaction paths.[5c−f] The solution folding of ubiquitin[6] involves an initial fast cooperative folding of the 23−34 α-helix and the 1−17 β-hairpin.[6a] In alcoholic solution an intermediate A state is observed,[6e,f] and three distinct states have also been found in the gas phase.[1c,g,2e] Earlier studies showed[7a−d] that intermolecular noncovalent complexes could survive the electrospray ionization (ESI) process by which ions are transferred from solution to the gas phase, and that the conformation in solution is a major factor in determining the charge state distribution of the gaseous ions.[7d−f] However, this does not require that the solution noncovalent bonding is retained in vacuo. If true, ESI/MS would provide a convenient screening method for combinatorial drug development,[7a−d] while, in fact, significant evidence to the contrary has been presented.[1−3]

The ECD capability for probing the conformational structure of gaseous protein cations is counter-intuitive; ECD dissociates covalent backbone bonds without appreciably affecting the far weaker noncovalent bonds. Capture of an electron at a protonated site is ∼6 eV exothermic; the relatively high H• atom affinity of a backbone carbonyl group leads to immediate (∼10^{-12} s, "nonergodic") dissociation, producing mainly (∼90%) ***c***,***z***• product ions (eq 1) with minor amounts of ***a***•,***y*** ions (eq 2).

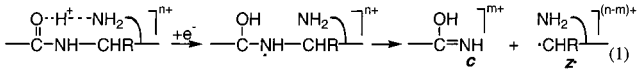

However, if the resulting two fragments from $(M + nH)^{n+}$ are still joined by noncovalent bonds, they will appear instead in the ECD spectrum as a reduced molecular ion, $(M + nH)^{(n-1)+\bullet}$, and are so considered here as "folded" products. Thus the abundances of the separated ("unfolded") eq 1 and eq 2 products relative to all folded products should be indicative of the unfolded/folded equilibrium.[3] As in solution, the effect of temperature on these values permits a van't Hoff evaluation of the corresponding unfolding enthalpies.[8]

In the first application of ECD conformational characterization to gaseous cytochrome *c* ions,[3] data could not be obtained from its heme region because of the competitive electron reduction there of Fe(III). In contrast, ions of the 76-residue non-heme ubiquitin can be extensively dissociated by ECD.[9] Its native structure and folding have been characterized by X-ray crystallography[10] and NMR spectroscopy,[11] showing closely similar structures in the solution and solid phases. In solution, its two-state cooperative unfolding has enthalpies between 180 and 300 kJ/mol for melting temperatures between 60 and 90 °C,[6] and an enthalpy value of ∼3000 kJ/mol (∼2500 kJ/mol H bonding and ∼500 kJ/mol van der Waals' interactions) was estimated for complete unfolding in a vacuum.[6d]

For gaseous ubiquitin ions formed by electrospray ionization, collisional cross sections identify compact (C), partially folded (P), and unfolded (U) conformers whose cross sections increase with increasing charge and temperature,[1c] although the extent of H/D exchange can decrease;[2a,e] ECD will be compared to these methods for characterization of different aspects of ion conformations.[3,4] A statistical study showed that ECD cleavages are largely nonspecific with respect to the identity of the adjacent amino acids,[4e] with the most definitive exception that ECD does not yield ***c***,***z***• products from cleavage on the N-terminal side of proline (as expected for its tertiary amide nitrogen from eq 1). This study extends other evidence[12] that formation of ECD product ions is also enhanced near protonation sites with secondary charge solvation, as well as inhibited by tertiary noncovalent bonding across a cleavage site.

Experimental Section

Experiments were performed on a 6T Fourier transform ion cyclotron resonance (FTICR) mass spectrometer described previously.[4] Bovine ubiquitin (Sigma, St. Louis, MO) was electrosprayed to produce specific charge state ions from solutions: 5+, 6+: 99:1 H_2O:NH_4OH; 7+, 8+: 99:1 H_2O:MeCOOH; 9+: 87:10:2:1 H_2O:MeOH:MeCOOH: glycerol; and 10+ to 13+: 49:49:2 H_2O:MeOH:MeCOOH. These ions were transferred into the FTICR ion cell through quadrupole ion guides, and decelerated and trapped with a nitrogen gas pulse (10^{-6} Torr peak pressure). In a typical temperature-effect experiment, the ions of interest were isolated employing SWIFT[13] waveforms and allowed to thermalize for 40 s, prior to irradiation with low-energy electrons (≤∼0.2 eV), dipolar excitation, and detection, averaging 20−25 scans (30−40 for the high-temperature spectra). Further, the 25−175 °C ECD spectra of the 7+ ions were measured separately three times and averaged. Kinetic unfolding/refolding experiments employed a pulsed (0.25 s) IR laser (10.6 μm),[3] followed at designated time intervals by a 1.2 s electron irradiation event to measure the ECD spectrum. Spectral interpretation utilized the automated THRASH program.[14] The peak intensity values are divided by the number of charges, as the ICR detector response is proportional to this number. Spectra were only recorded above *m*/*z* 845 (6+ ions), 740 (10+), 640 (11+), 600 (7+ to 9+), and 400 (12+, 13+), so that data for cleavages near the termini were obtained only for the larger of the two fragment ions (eqs 1 and 2).

Results

Determination of *K*(unfolding). A thermally induced order−disorder transition can be monitored, at an appropriate wave-

(5) (a) Baldwin, R. L. *J. Biomol. NMR* **1995**, *5*, 103−109. (b) Rumbley, J.; Hoang, L.; Mayne, L.; Englander, S. W. *Proc. Natl. Acad. Sci. U.S.A.* **2000**, *98*, 105−112. (c) Lazaridis, T.; Karplus, M. *Science* **1997**, *278*, 1928−1931. (d) Bryngelson, J. D.; Onuchic, J. N.; Socci, N. D.; Wolynes, P. G. *Proteins: Struct. Funct., Genet.* **1995**, *21*, 167−195. (e) Dill, K. A. *Protein Sci.* **1999**, *8*, 1166−1180. (f) Dinner, A. R.; Sali, A.; Smith, L. J.; Dobson, C. M.; Karplus, M. *Trends Biochem. Sci.* **2000**, *25* 331−339.
(6) (a) Briggs, M. S.; Roder, H. *Proc. Natl. Acad. Sci. U.S.A.* **1992**, *89*, 2017−2021. (b) Wintrode, P. L.; Makhatadze, G. I.; Privalov, P. L. *Proteins: Struct. Funct. Genet.* **1994**, *18*, 246−254. (c) Ibarra-Molero, B.; Loladze, V. V.; Makhatadze, G. I.; Sanchez-Ruiz, J. M. *Biochemistry* **1999**, *38*, 8138−8149. (d) Makhatadze, G. I.; Privalov, P. L. *Adv. Protein Chem.* **1995**, *47*, 307−425. (e) Woolfson, D. N.; Cooper, A.; Harding, M. M.; Williams, D. H.; Evans, P. A. *J. Mol. Biol.* **1993**, *229*, 502−511. (f) Jourdan, M.; Searle, M. S. *Biochemistry* **2001**, *40*, 10317−10325. (g) Zweckstetter, M.; Bax, A. *J. Am. Chem. Soc.* **2001**, *123*, 9490−9491.
(7) (a) Ganem, B.; Li, Y.-T.; Henion, J. D. *J. Am. Chem. Soc.* **1991**, *113*, 6294−6296. (b) Cheng, X.; Chen, R.; Bruce, J. E.; Schwartz, B. L.; Anderson, G. A.; Hofstadler, S. A.; Gale, D. C.; Smith, R. D.; Gao, J.; Sigal, G. B.; Mammen, M.; Whitesides, G. M. *J. Am. Chem. Soc.* **1995**, *117*, 8859−8860. (c) Jorgensen, T. J. D.; Roepstorff, P.; Heck, A. J. R. *Anal. Chem.* **1998**, *70*, 4427−4432. (d) Loo, J. A. *Int. J. Mass Spectrom.* **2000**, *200*, 175−186. (e) Katta, V.; Chait, B. T. *J. Am. Chem. Soc.* **1991**, *113*, 8534−8535. (f) Konermann, L.; Douglas, D. J. *Biochemistry* **1997**, *36*, 12296−12302. (g) Nesatyy, V. J. *J. Mass Spectrom.* **2001**, *36*, 950−959.
(8) Marky, L. A.; Breslauer, K. J. *Biopolymers* **1987**, *26*, 1601−1620.
(9) Horn, D. M.; Zubarev, R. A.; McLafferty, F. W. *Proc. Natl. Acad. Sci. U.S.A.* **2000**, *97*, 10313−10317. Sze, S. K.; Ge, Y.; Oh, H. B.; McLafferty, F. W. *Proc. Natl Acad. Sci. U.S.A.* **2002**, *99*, 1774−1779.
(10) Vijay-Kumar, S.; Bugg, C. E.; Cook, W. J. *J. Mol. Biol.* **1987**, *194*, 531−544.
(11) (a) DiStefano, D. L.; Want, A. J. *Biochemistry* **1987**, *26*, 7272−7281. (b) Weber, P. L.; Brown, S. C.; Mueller, L. *Biochemistry* **1987**, *26*, 7282−7290.
(12) Cerda, B. A.; Breuker, K.; Horn, D. M.; McLafferty, F. W. *J. Am. Soc. Mass Spectrom.* **2001**, *12*, 565−570.
(13) Marshall, A. G.; Wang. T. C. L.; Ricca, T. L. *J. Am. Chem. Soc.* **1998**, *107*, 7893−7897.
(14) Horn, D. M.; Zubarev, R. A.; McLafferty, F. W. *J. Am. Soc. Mass Spectrom.* **2000**, *11*, 320−332.

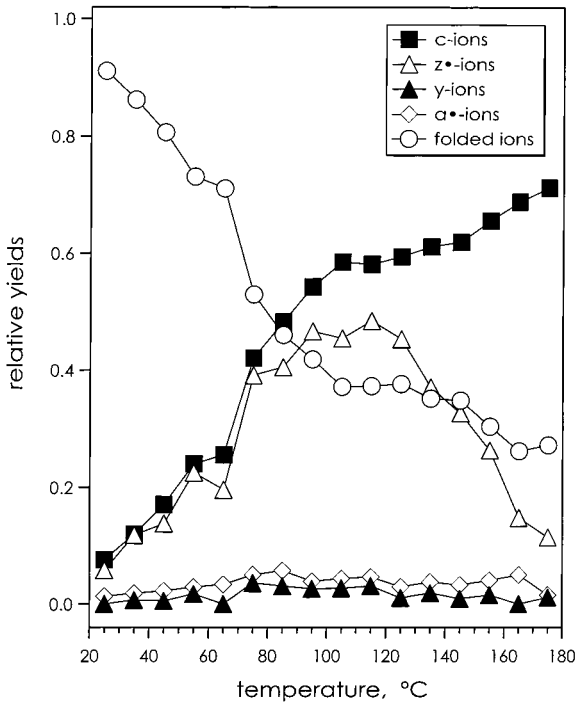

Figure 1. Relative yields as a function of temperature of ***c***, ***z•***, ***a•***, and ***y*** fragment ions and folded ions (see Results for definition) produced by electron capture of $(M + 7H)^{7+}$ ubiquitin ions.

length, by the change in UV absorbance with increasing temperature, a "UV melting curve".[7] For the determination of thermodynamic data, the absorbance must be directly related to the fraction of the unfolded species under thermal equilibration, *K*(unfolding) = [unfolded]/[folded]. Applying this to the ECD of gaseous ions, the [unfolded] value at a specific interresidue site (eqs 1 and 2) is indicated by the ion abundances $[(\boldsymbol{c} + \boldsymbol{z}^{\bullet})/2] + [(\boldsymbol{a}^{\bullet} + \boldsymbol{y})/2]$; this assumes that the e^- capture indicated by $(M + nH)^{(n-1)+\bullet}$ in the spectrum actually produces fragment ion pairs (eqs 1 and 2), but that these are still held together by the original noncovalent bonding.

Is it probable that an unfolded $(M + nH)^{n+}$ precursor ion can capture an electron without undergoing backbone dissociation? RRKM calculations on the simple system of $H^{\bullet}$ captured on the carbonyl of *N*-methyl acetamide indicated that this radical species is unstable, with the only alternative dissociation channel as the reversal loss of $H^{\bullet}$ at lower energies.[4b] $H^{\bullet}$ loss is a minor process,[16] and Figure 1 shows a 70% yield of ***c*** ions from ECD of 7+ ions at 175 °C. In addition, the $(M + 7H)^{6+\bullet}$ reduced ions formed from electron capture by the $(M + 7H)^{7+}$ ions can be extensively (>90%) dissociated by IRMPD; both this and SORI/CAD produce the ***c***,***z•*** fragment ions (eq 1) found in the ECD 7+ spectra of Figure 1. This also requires only ~10% of the RF power required for a comparable CAD of the $(M + 7H)^{7+}$ ions, consistent with cleavage of noncovalent bonds in the dissociation of $(M + 7H)^{6+\bullet}$ ions. The validity of the *K*(unfolding) determination will be tested below, such as by comparing the ECD results to the ion collision cross section data (Figure 2).

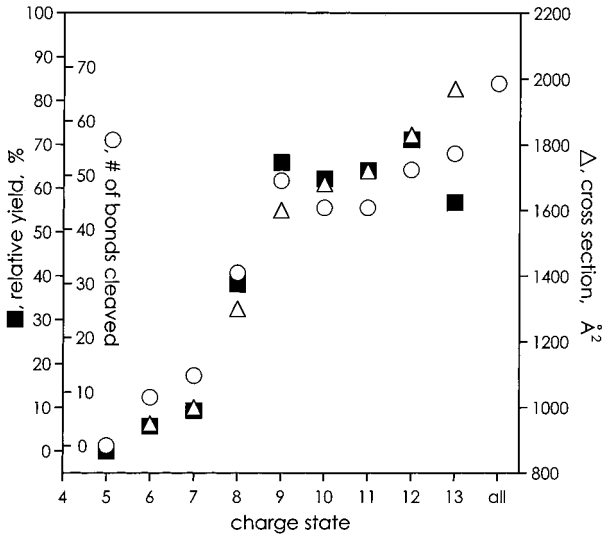

Figure 2. Normalized yield of ECD fragment ions (filled squares), number of backbone bonds cleaved by ECD (open circles), and collisional cross sections (open triangles) determined in ion mobility experiments (ref 1c, Figure 3, solid lines) for ubiquitin parent ion charge states 5+ to 13+. The calculated ion mobility cross sections for the crystal and near-linear conformers are 920 and 2150 Å^2.

As shown by ECD of 7+ ions (Figure 1), the radical ***z•*** ions are unstable above ~100 °C (6+, 8+, and 9+ ions show similar behavior).[15] The radical ***a•*** ions are far more stable (and ***y*** ions can also be adventitiously formed by collisionally activated dissociation, CAD, or blackbody infrared radiative dissociation, BIRD), so that $[\boldsymbol{c} + \boldsymbol{a}^{\bullet}]$ is generally used here for the [unfolded] value. For cleavages near the N-terminus where low mass ***c*** ions were not recorded or were of far lower signal/noise than their more highly charged ***z•*** counterparts, ***z•*** ions were also used appropriately. With increasing temperature the ECD spectra show peak intensities corresponding to the increasing loss of small neutral species (e.g., $HO^{\bullet}$, $HCO_2^{\bullet}$) from the reduced molecular ion $(M + nH)^{(n-1)+\bullet}$, so that the total intensity of these secondary products is included in the [folded] value as an approximate replacement for the $(M + nH)^{(n-1)+\bullet}$ ions lost.[16]

Discussion

General Similarity of Ion Mobility and ECD Data. As found for cytochrome *c* ions,[17] the average ion collision cross sections for ubiquitin ions determined by Clemmer and co-workers[1c] (and confirmed by Guevremont and co-workers)[1g] increase with increasing charge (Figure 2), consistent with increased denaturation and electrostatic repulsion.[18] However, H/D exchange values (corrected for exchanged protons) actually decrease from 6+ to 13+,[2a,e] consistent with an offsetting

(15) The analogous glycine *N*-methylamide radicals undergo facile dissociation by several reactions: Turecek, F.; Carpenter, F. H. *J. Chem. Soc., Perkin Trans. 2* **1999**, 2315−2323.

(16) The isotopic peaks of the $(M + nH)^{(n-1)+\bullet}$ ions are not distinguished in these measurements from those of the even-electron $H^{\bullet}$ loss products $[M + (n - 1)H]^{(n-1)+}$. RRKM calculations show that $H^{\bullet}$ loss can be a competitive nonergodic dissociation.[4b] Separate 25 °C experiments for ECD of monoisotopically selected $(M + nH)^{n+}$ ions show that the proportion of $H^{\bullet}$ loss product, versus the reduced species, is as follows: 7+, 4%; 8+, 7%; and 9+, 29%; at 170 °C it is ~100%. Further, at higher charge states, an appreciable extent of e^- capture is not accompanied by backbone fragmentation, apparently due to the stable α-helical structure: Breuker, K.; Oh, H. B.; Cerda, B. A.; Horn, D. M.; McLafferty, F. W. *Eur. J. Mass Spectrom.* **2002**, *8*, 177−180.

(17) Shelimov, K. B.; Clemmer, D. E.; Hudgins, R. R.; Jarrold, M. F. *J. Am. Chem. Soc.* **1997**, *119*, 2240−2248.

(18) For the compact (C), partially folded (P), and unfolded (U) states identified by Clemmer and co-workers,[1c] approximate melting temperatures derived from their data (ESI of 49:49:2 H_2O:MeCN:MeCOOH) for C → P and P → U, respectively, are as follows: 6+, 80 and 110 °C; 7+, 50 and 90 °C; 8+, <25 and 85 °C; and 9^+, <25 and 80 °C. Full unfolding (~100% U) is reached for 7+ at 140 °C; 8+ at 120 °C; 9+ at 100 °C; and 10+ at 80 °C.

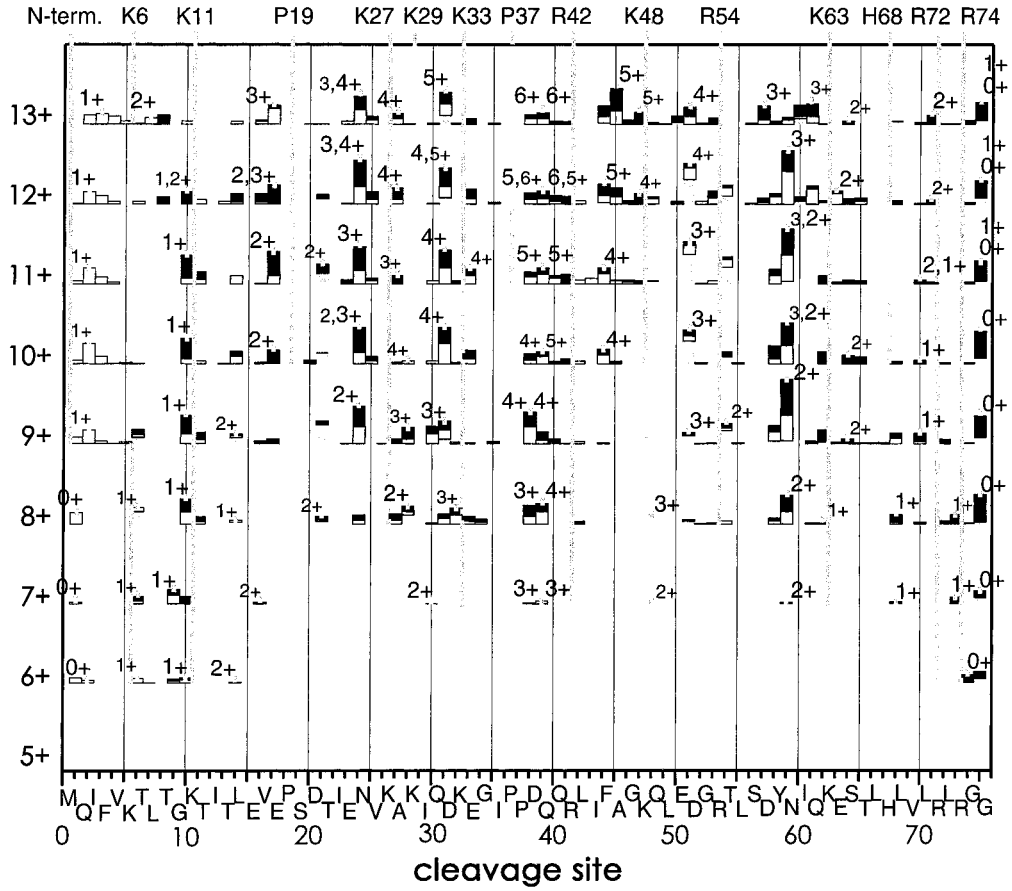

Figure 3. Normalized abundances (vertical bars) of separated ECD dissociation products versus cleavage site for parent ion charge states 5+ to 13+. Black segment (top of vertical bar), ***c*** ions; open segment, $z^{\bullet}$ ions; gray segment, $a^{\bullet} + y$ ions. Vertical stripes below the protonation sites indicate the most probable sites (dashed stripes, shared probability) based on the charge states of ***c***, $z^{\bullet}$ products from nearby ECD cleavages; only three of the six sites are predicted for the 6+ ions.

increase in secondary structure involving solvation of the new protonated side chain to a backbone carbonyl; experimental evidence for this explanation has been offered for cytochrome *c* ions.[2d] The relative ECD yield of unfolded ions at 25 °C not only increases in general with increasing charge state (Figure 2), as does the number of backbone bonds cleaved by ECD, but these changes correlate surprisingly well with the average ion collision cross section data for ions electrosprayed under similar conditions.[1c] Apparently the ion's tertiary noncovalent structure is similarly effective in reducing its cross section and in preventing separation of the products of eqs 1 and 2. From theoretical calculations, the 13+ ion cross section value corresponds to "unfolded conformations with little tertiary structure";[1c] the 13+ ECD spectrum is unchanged by heating the ions to 125 °C, consistent with no remaining tertiary noncovalent bonding at room temperature.

The Unique 13+ Conformers. The 25 °C ECD spectra (Figure 3) of the 5+ to 13+ ubiquitin ions indicate that the bond cleavages of the 13+ ions are substantially different than those of the other charge values. In a comparison of the relative ECD intensities of the fragment ions of the 11+ and 13+ ECD spectra (Figure 4), nearly half of the mass values show a poor abundance correlation. On the other hand, plotting the average abundance values of 11+ and 13+ spectra versus those for the 12+ spectrum provides strong evidence that the 12+ ion population represents a mixture of 11+ and 13+ conformers of approximately equal abundance. This is in very good

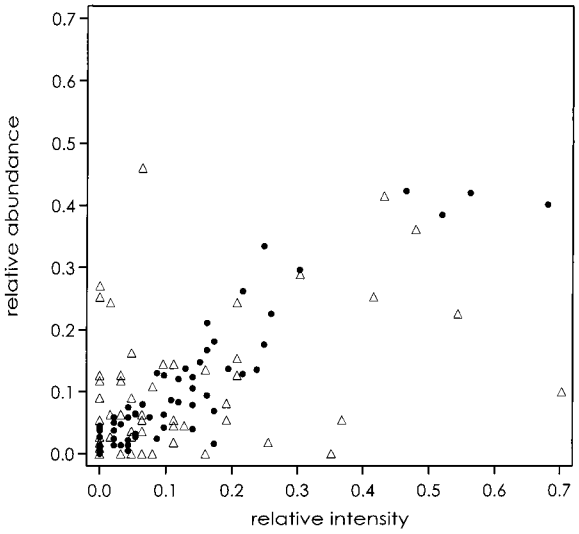

Figure 4. Correlation to compare normalized abundances of Figure 3 ECD spectra: open triangles, $(M + 13H)^{13+}$ (*y* axis) versus $(M + 11H)^{11+}$ data; filled circles, average of $(M + 13H)^{13+}$ and $(M + 11H)^{11+}$ data (*y* axis) versus $(M + 12H)^{12+}$ data.

agreement with gas-phase H/D exchange results first obtained by Cassady and co-workers.[2b] Proton-transfer reactivity studies indicate that the 13+ ions have a structure similar to one, but not the other, fraction of the 12+ population.[1a]

The extensive H/D data of Marshall and co-workers[2e] also suggest that one isomeric form of the 12+ ions (exchanging

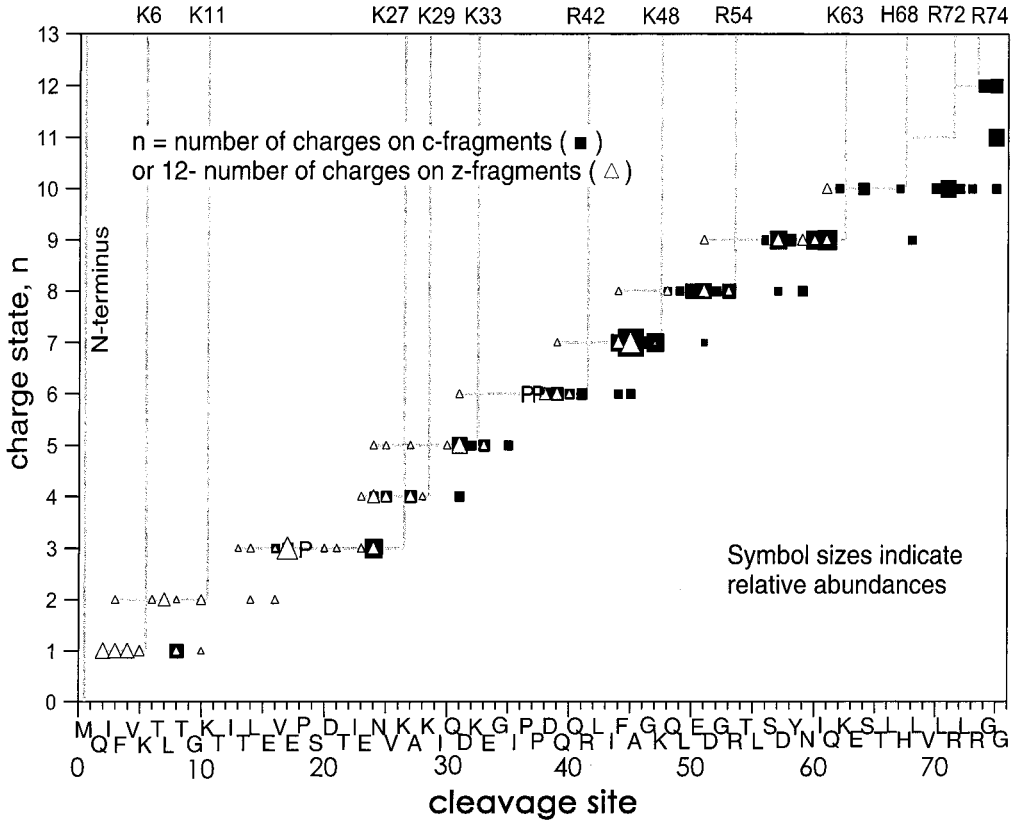

Figure 5. Fragment ion charge states for the ECD spectrum of the $(M + 13H)^{13+}$ ions.

14 D in addition to those replacing the 12 protons) is similar to that of the 13+ ion population (exchanging no additional D atoms), and that the other 12+ fraction (exchanging an additional 38 D) is similar to the 11+ ion structure (exchanging an additional 50 D). For cytochrome *c*, however, increasing a conformer's charge value by one decreased the number of exchangeable hydrogens by only two, presumably by backbone solvation of the newly charged side chain to protect two sites, on average, from secondary intramolecular exchange after the primary H/D exchange of a proton. For the 11+ to 13+ ubiquitin ions, one additional charge appears to prevent exchange at 12 to 14 sites,[2e] suggesting that this charge causes a far more serious interference with secondary intramolecular exchange. The 13+ ions exchanged 13 D atoms in total;[2e] as demonstrated for cytochrome *c* ions,[2d] intermolecular H/D exchange at protonation sites should be favored, so that zero additional sites would have undergone intramolecular exchange. This charge solvation would have completely immobilized the original D+ replacements, even preventing further intermolecular exchange, such as on a Lys-NH_2D^+ site. Alternatively, intermolecular H/D exchange at central protonated sites could be prevented by the strong proton solvation to the backbone, with the 13 D representing multiple H/D exchange at basic residues near the termini.

Recent ion collision cross section data indicate that the 13+ ions do not represent a single conformer.[1h] These data for the 11+ to 15+ ubiquitin ions indicate multiple conformers that are proposed to have their protonated sites in different locations;[1h] these would thus also represent isomeric variants. The 13+ to 15+ ions have nearly identical (1942−2020 Å^2) cross sections, suggesting that all these have a "near linear" conformation;[1h] changing the position of a side chain solvation should have only a local effect on the secondary structure, and thus have little effect on the collision cross section. Despite the absence of tertiary noncovalent bonding (vide supra), the 13+ ECD spectrum still shows regions in which cleavages do not occur, suggesting a role also for secondary ion structure in directing ECD cleavages.

Charge Distribution in Ubiquitin Ions. The charge values of the ECD $\boldsymbol{c}$,$\boldsymbol{z}^\bullet$ products of the 13+ ions, in which all the basic Lys (K), Arg (R), and His (H) residues and the N-terminus should be protonated,[19] are shown in Figure 5. Cleavage at bond 39 of this 76-residue ion yields exclusively $\boldsymbol{c}^{6+}$ and $\boldsymbol{z}^{\bullet 6+}$ from $(M + 13H)^{13+}$; this would correspond to e^- capture at the central R42 protonated site, as there are six charge sites on either side of R42. This is indicated in the Figure 3 ECD 13+ spectrum by "6+⊥6+" on either side of the bond 39 cleavage. Similarly, any cleavage of a 13+ ion after e^- neutralization will give a $\boldsymbol{c}^{n+}$ ion and a $\boldsymbol{z}^{\bullet(12-n)+}$ ion. Plotting the 13+ product cleavage sites versus their *n* values (Figure 5) shows that most cleavage sites are only a few residues away, usually toward the N-terminus, from the charge site at which the electron has apparently been captured.[20] This charge site correlation was observed for poly(ethylene glycol) multiply charged cations.[12] It is consistent with the postulate[4b,c] that ECD proceeds through e^- capture to generate a high-*n* Rydberg state,[21] which undergoes an avoided crossing to the final state dissociative surface that has the neutralized proton attached to the carbonyl oxygen. Thus

(19) Schnier, P. D.; Gross, D. S.; Williams, E. R. *J. Am. Soc. Mass Spectrom.* **1995**, *6*, 1086−1097.

(20) The same, but less abundant, product ion formed in a lower charge state could arise by capture of a second electron. Thus the $\boldsymbol{c}_{44}{}^{6+}$ (C-terminal side of other $\boldsymbol{c}^{6+}$ ions) and $\boldsymbol{z}^{\bullet}{}_{32}{}^{4+}$ (N-terminal side of other $\boldsymbol{z}^{\bullet 4+}$ ions) products could arise from reduction of the complementary $\boldsymbol{c}_{44}{}^{7+}$ and $\boldsymbol{z}^{\bullet}{}_{32}{}^{5+}$ ions. Note that the probability for e^- capture is proportional to the square of the charge value.[4]

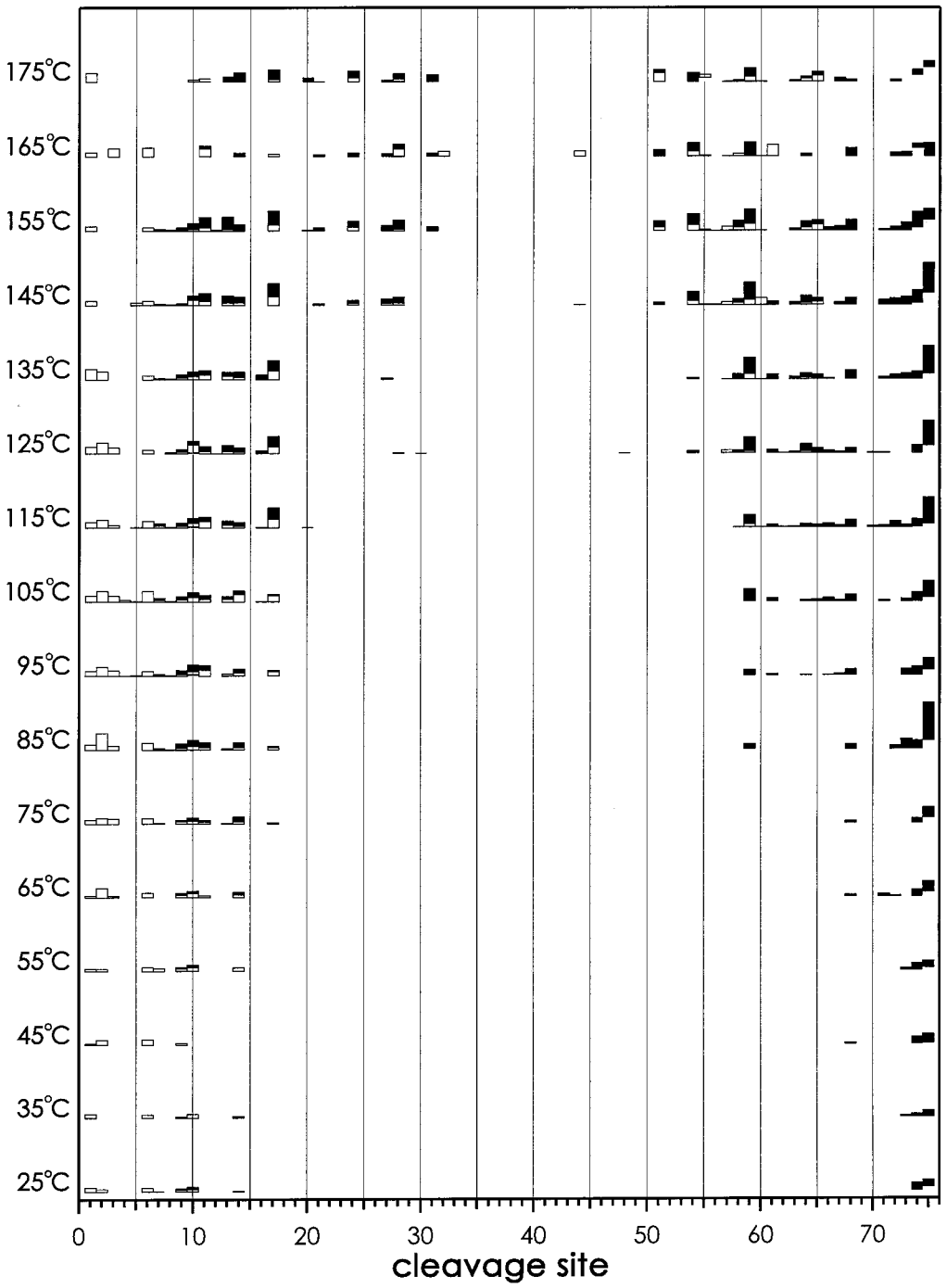

Figure 6. ECD spectra of $(M + 6H)^{6+}$: normalized abundances of separated dissociation products versus cleavage site for temperatures 25−175 °C. Notation as in Figure 3.

the reaction intermediate that precedes surface crossing should have the proton on a protonated side chain adjacent to the carbonyl oxygen, with the Figure 5 data consistent with this proton positioned to balance the overall electrostatic forces of the multiple charges.

Thus the Arg72 and Arg74 protons have apparently been repelled toward the C-terminal end to initiate attack on the carbonyl groups resulting in cleavage of bonds 74 and 75, while the His68 proton has similarly caused cleavages from bonds 61 to 75 (although the cleavages at bonds 70−75 could also arise from secondary electron capture).[20] On the other hand, the data appear to indicate that the protonated Lys27 has led to cleavages as far away as bonds 14, 16, and 17. Here, the charge distributions for the gaseous 13+ ubiquitin ions calculated by Williams and co-workers[19] indicate a substantial protonation probability at Pro19 (Figure 3), much greater than that at Lys29; an α-helix model indicates that an H^+ on the tertiary amide N atom of Pro19 would be near the carbonyl groups of residues 17 and 16.

(21) Siu Kwan Sze points out that for the "dissociative recombination reaction" of an electron with a simple ion such as H_3O^+, early workers postulated a now well-accepted mechanism with initial formation of a high-*n* Rydberg state that transfers to a repulsive state that then immediately dissociates: Huang, C.-M.; Whitaker, M.; Biondi, M. A.; Johnsen, R. *Phys. Rev. A* **1978**, *18*, 64−67. Datz, S. *J. Phys. Chem. A* **2001**, *105*, 2369−2373.

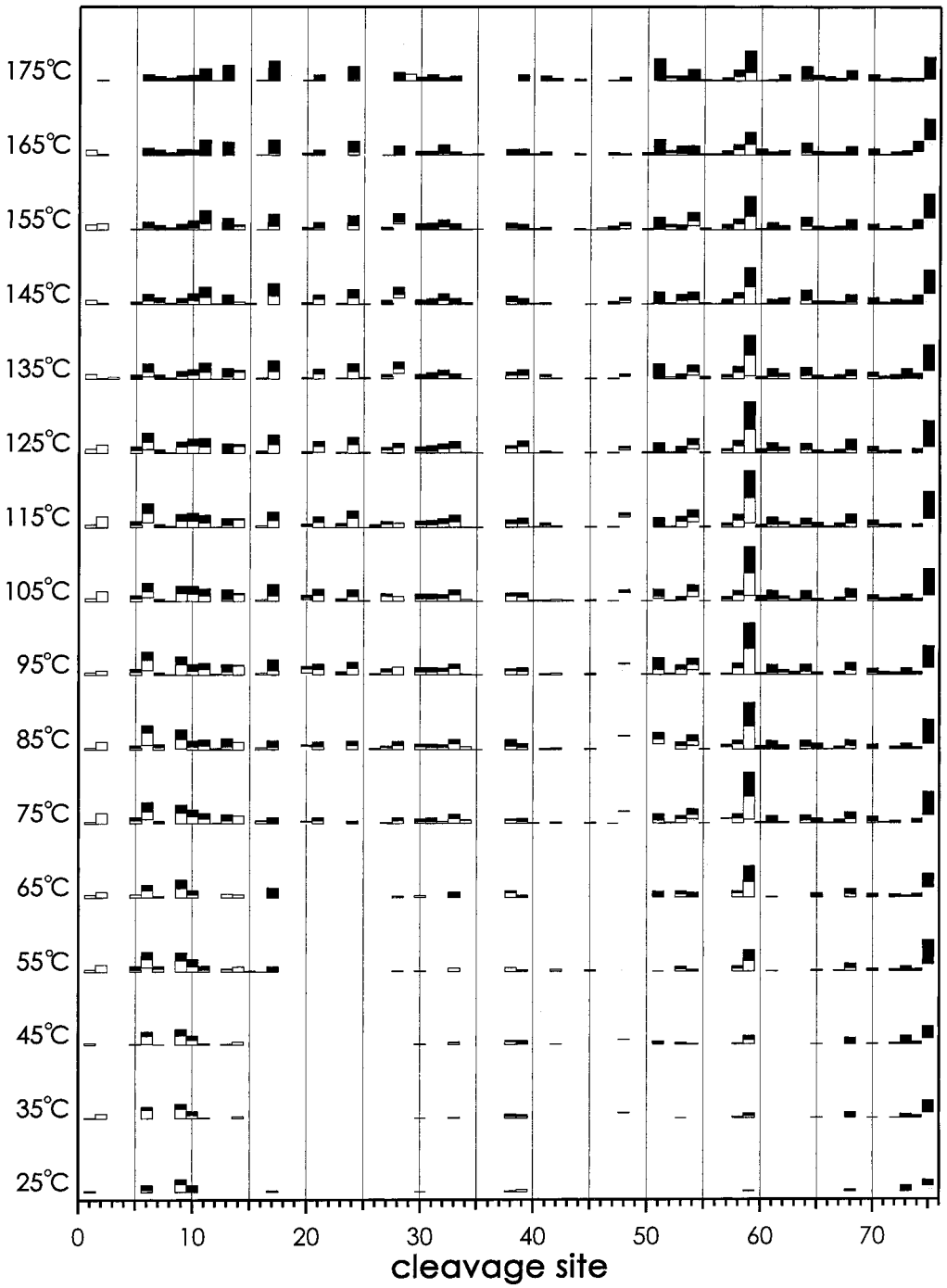

Figure 7. ECD spectra of $(M + 7H)^{7+}$, as in Figure 6.

The same type of product ion charge data was used to assign (Figure 3, vertical stripes) the most probable protonated sites for the 7+ to 13+ ions, with dashed vertical stripes indicating partial charging. The protonation probabilities calculated by Williams and co-workers[19] for the 7+ ions are highest (in decreasing order) for R42, R54, K11, R74, K27, K6, and K33 (with K63 and H68 nearly as high); the ECD data (Figure 3) indicate five of these basic residues for 7+ ions, but replaced R54 and K27 with K63 and R72. As discussed further below, tertiary noncovalent bonding in the central region should bring its basic residues closer together and displace proton density toward the termini. The dashed vertical stripes of Figure 3 also indicate that multiple isomers, protonated at different sites,[19] are possible for each charge state, consistent with the multiple cross section values for the 11+ to 15+ ubiquitin ions.[1h]

The Near-Linear 13+ Conformers. Thus the cross section[1c,h] and H/D exchange[2e] data combined with this ECD evidence indicates that the 13+ ubiquitin ions have no tertiary noncovalent bonding; these are "near linear" conformers[1h] stabilized by backbone solvation of the protonated side chains.[2d] This solvation appears to provide a local structure closely resembling the intermediate structure required for ECD that induces cleavage one to six residues away, possibly with a helical conformation[22] that is given further rigidity by the solvated side chains.[16] In solution, increasing the degree of protonation (i.e., acidity) destroys the secondary as well as the tertiary nonco-

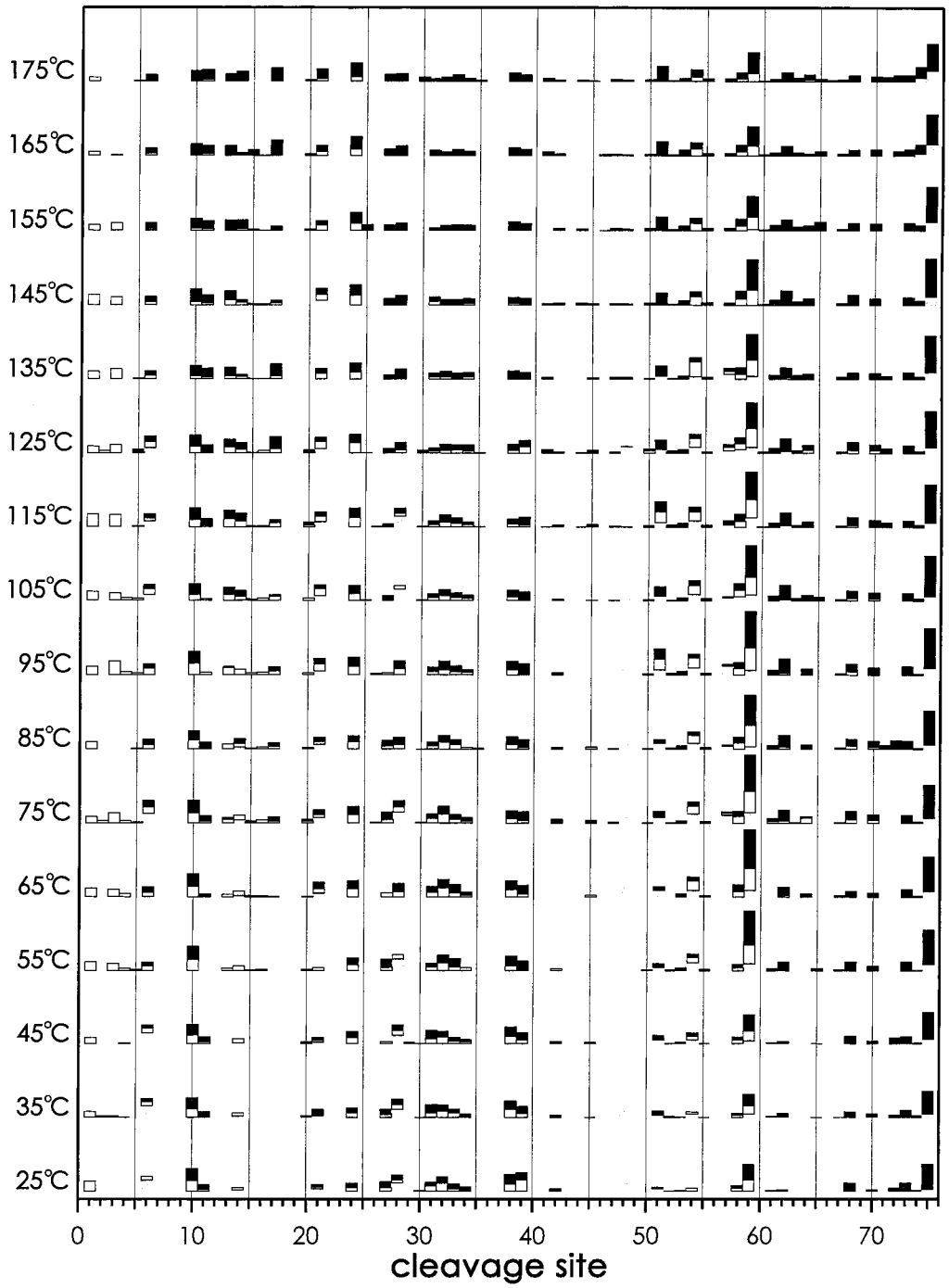

Figure 8. ECD of $(M + 8H)^{8+}$, as in Figure 6.

valent structure, with the added side chain protons solvated into the exterior aqueous phase. Removal of this phase has the opposite effect, with the newly protonated side chains making the conformer so rigid that secondary (or, possibly, even primary) H/D exchange is dramatically decreased in the 13+ ions.[2e]

Ion Charge State versus Unfolding. At 25 °C, ECD of 5+ ubiquitin ions yields no separated backbone cleavage products; all backbone sites appear to be held together by noncovalent bonding. Similarly, CAD, infrared multiphoton dissociation, and BIRD of 5+ ubiquitin ions cause only small molecule (e.g., H_2O) loss.[23] Figure 3 indicates that the 6+ and 7+ ions are mainly compact, only unfolded at the N- and C-termini where the charge density appears to be highest. The 8+ and 9+ ions are much more extensively unfolded. Some further unfolding, such as to produce cleavage at bond 44, is shown by the ECD spectrum of the 10+ ions, while cleavages at bonds 45−47 only appear for more highly charged ions. Reasons for the high stability of the 44 to 47 bond region are not obvious; the nearest

(22) Hudgins, R. R.; Ratner, M. A.; Jarrold, M. F. *J. Am. Chem. Soc.* **1998**, *120*, 12974−12975. Hudgins, R. R.; Jarrold, M. F. *J. Am. Chem. Soc.* **1999**, *121*, 3494−3501.

(23) Senko, M. W.; Speir, J. P.; McLafferty, F. W. *Anal. Chem.* **1994**, *66*, 2801−2808. Little, D. P.; Speir, J. P.; Senko, M. W.; O'Conner, P. B.; McLafferty, F. W. *Anal. Chem.* **1994**, *66*, 2809−2815. Reid, G. E.; Wu, J.; Chrisman, P. A.; Wells, J. M.; McLuckey, S. A. *Anal. Chem.* **2001**, *73*, 3274−3281.

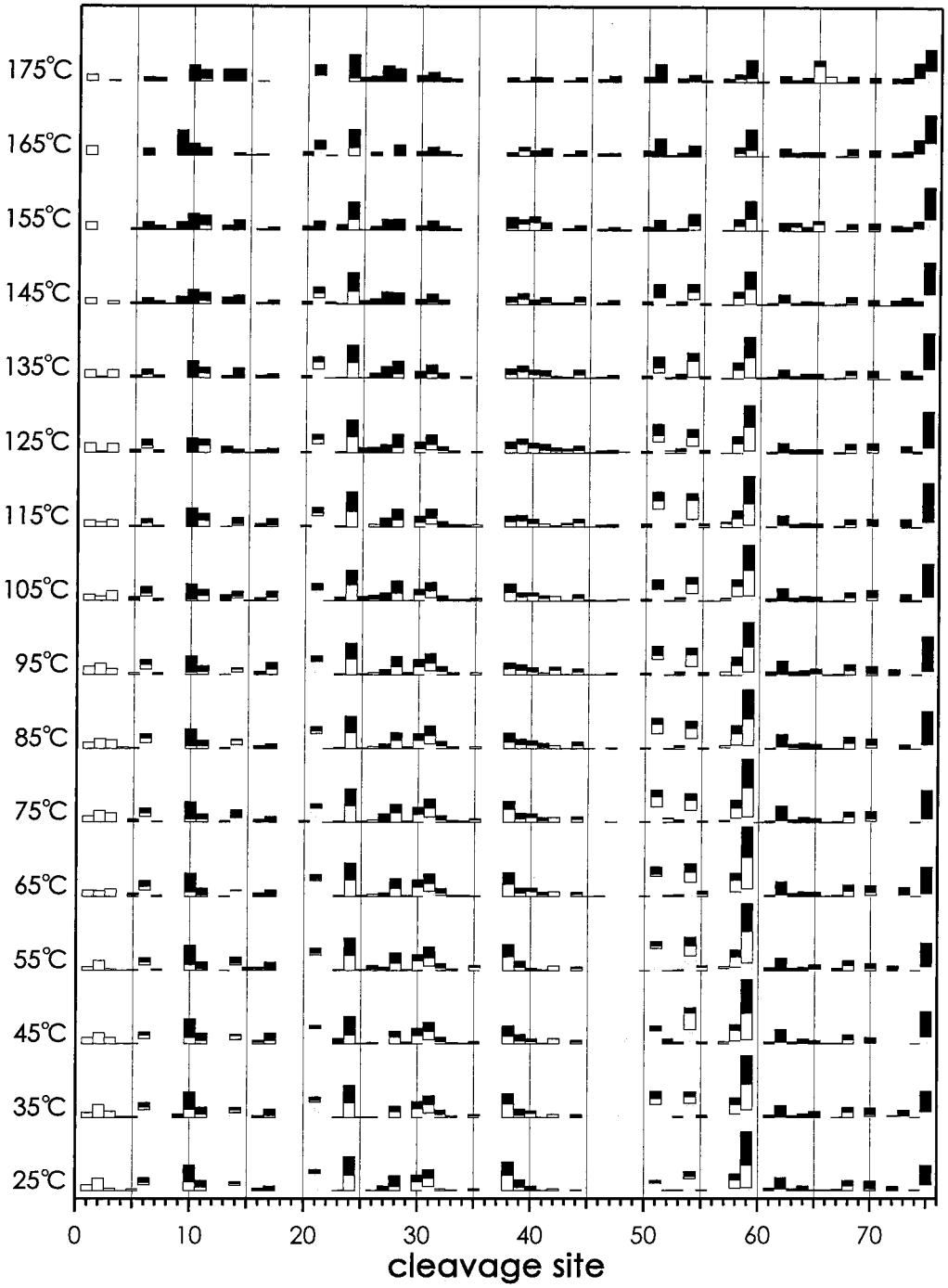

Figure 9. ECD of $(M + 9H)^{9+}$, as in Figure 6.

salt bridges could involve Asp44, Glu50, and/or Asp51 with Arg42 and Lys48. As portrayed in the Table of Contents graphic, increasing the ionic charge from 5+ to 13+ appears to break first the tertiary bonding between the termini, then between (approximately) residues 11 and 72, then between 11 and 26 plus between 50 and 58, then between 15 and 20 plus between 40 and 45, and finally between 45 and 50.

Folding in solution has been shown to proceed through a fast (~8 ms) cooperative event that forms the 23−34 α-helix and the 1−17 β-hairpin,[6a] stabilized by hydrophobic bonding between these secondary structures. Alcoholic solution folding yields an A state with N-terminal α-helical and β-sheet structures and C-terminal non-native α-helical structures;[6e,f] the gas-phase folding induced by removing protons shows no apparent relationship to either behavior in solution. This folding dichotomy was also found for cytochrome *c*, consistent with the decreased hydrophobic effect in the gas phase.[2d,3] The ECD products from cleavage of bonds 44 to 47 are separated only in the highest charge states, while this is part of an exterior loop in the native structure. As a further contrast, the gaseous 13+ ions fold to additional near-linear conformers.[1h]

Overall Unfolding Enthalpy. The largest changes in conformation with change in charge state occur for the 6+ to 9+ ions (Figures 2 and 3), so that their ECD spectra were determined at 10° intervals from 25 to 175 °C (Figures 6−9).[24] In total, ECD has been able to effect cleavages at all interresidue

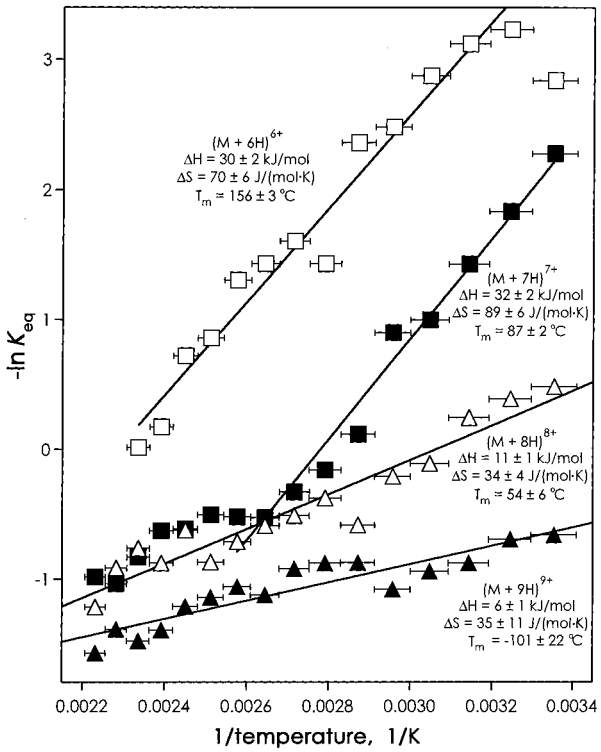

Figure 10. van't Hoff plot, ln K_{eq} versus $1/T$ for K(unfolding) = [unfolded]/[folded], for the ECD data of Figures 6−9. Individual ΔS values derived from these data (not shown) are mostly 50−400 J/(mol K), but with large experimental errors.

bonds except 15, 22, and 69, plus 18, 36, and 37 whose cleavage is prevented by adjacent proline residues.[4] The ions were first stored for 40 s in the heated vacuum chamber of the FT-ICR instrument to establish thermal equilibrium using blackbody infrared radiation.[25a] The enthalpy change (ΔH) of unfolding (see Results), neglecting any temperature dependence on ΔH, is indicated by a van't Hoff analysis (Figure 10).[8] For the summed [$\boldsymbol{c} + \boldsymbol{a}^{\bullet}$] values for ECD of 6+ ions, and of 7+ ions up to ~100 °C, the data indicate a single unfolding enthalpy of ~31 kJ/mol. The unfolding of 8+ and 9+ ions, and of the 7+ ions above 100 °C, shows lower ΔH values of ~6−11 kJ/mol. These enthalpy requirements are far lower than the 160−300 kJ/mol measured in aqueous solution;[6] the native → A state unfolding of the tertiary structure shows similarly high values.[6f] Thus unfolding in the gas phase of the tertiary structure shows only 13−25% of the enthalpy of that in solution of the native structure designed by natural selection for high stability. The enthalpy for complete unfolding of the native conformer in vacuo was estimated as ~3000 kJ/mol.[6d] The far lower values of ΔH(unfolding) measured here are consistent with the loss of hydrophobic bonding in the gaseous ions, as well as the fact that the unfolding of the tertiary structure that is produced by protonation is offset by the formation of a secondary (helical?) structure.

Williams and co-workers (as confirmed by Marshall and co-workers) have determined Arrhenius activation parameters for CAD of ubiquitin ions,[25] with very similar values of activation energy (E_{act}) and log A values, respectively, for charge state pairs: 6+, 7+: 0.96 eV and 9.4; 8+, 9+: 1.20 eV and 11.9; and 10+, 11+: 1.55 eV and 16.5 (note that the ECD spectra of Figure 3 are also the most similar for the same charge state pairs). The increases in E_{act} with increasing charge 6+ to 9+ reflect in part the ΔH(unfolding) of 0.4 eV found here; the overall increase to 11+ includes the energy necessary to dissociate the additional secondary structure resulting from backbone solvation of the additional protonated side chains,[2d] as discussed above for the 13+ ions. The dramatic increases in these A values are in qualitative agreement with the decreased C → P and P → U unfolding entropies.

Pulsed Laser Unfolding and Refolding. For the 25 °C 7+ ubiquitin ions, a 0.25 s photoexcitation pulse from a continuous IR laser[3] produces a rapid abundance increase in many fragment ions of the ECD spectrum (Figures 11 and 12); the new spectrum is quite similar to the ECD spectra at 75−95 °C (Figure 7),[26] corresponding to C → P unfolding (Figure 10). Electron irradiation of the ions was started 0.07 s after the IR pulse and continued for 1.2 s, so that the "0.07 s" ECD spectrum represents an integration of the spectra of conformer states present over this 1.2 s period. Despite this, the "0.17 s spectrum", a 1.2 s measurement started 0.17 s after the laser pulse, shows significant abundance decreases (and thus refolding) versus the 0.07 s spectrum. Most unfolding, as well as the IR activation, has required ≤0.1 s (Figure 12); in a similar experiment, unfolding of the larger gaseous 15+ cytochrome *c* ions required >5 s.[3]

Refolding rate constants are surprisingly similar at the major backbone sites of bonds 14, 24, 51, and 54 (log plot, Figure 12); other sites originally showing a low cleavage probability such as 5, 11, 16, 21, 28, 32, 39, 53, 58, 61, 64, and 72 are also mostly folded in 1 s. The experiment was repeated with the 7+ ions trapped in the ICR cell now heated to 65 °C (Figure 13). This displaces the equilibrium to far higher proportions of unfolding at each of these sites before the pulsed excitation and slows the refolding at bond 24 substantially (Figure 12), and that at bond 51 even more. This resembles the "slower" refolding of the 25 °C ions at bonds 48, 59, and 68, all of which give more abundant peaks in the 7+ 25 °C ECD spectrum. However, the rate of refolding of just the fraction of these conformers unfolded by the laser pulse is obviously higher, more consistent with the faster refolding rates of Figure 12. The most favored ECD cleavages show minimal effects of laser excitation, consistent with minimal tertiary noncovalent bonding at these locations.

Thus part, but not all, of the refolding of 7+ ions involves cooperative P → C formation of the compact structure. Longer term cooling under collision-free conditions at room temperature (Figure 12) caused further folding at some bonds (vide infra), and even showed unfolding at bond 68 in repeated spectra; for 15+ cytochrome *c* ions, noncovalent bonding at many sites continued to unfold for 60 s after pulsed laser excitation.[3]

The same conditions of pulsed IR gave no discernible change in the spectra of 25 °C 9+ ions (data not shown), reflecting the minimal spectral change in heating the 9+ ions to 75−95 °C (Figure 9).

(24) Signal/noise for the 165° and 175° spectra for the 6+ ions is poor because of large H_2O losses from BIRD, as observed by Williams and co-workers.[25a]

(25) (a) Jockusch, R. A.; Schnier, P. D.; Price, W. D.; Strittmatter, E. F.; Demirev, P. A.; Williams, E. R. *Anal. Chem.* **1997**, *69*, 1119−1126. (b) Freitas, M. A.; Hendrickson, C. L.; Marshall, A. G. *J. Am. Chem. Soc.* **2000**, *122*, 7768−7775.

(26) The pulsed laser data of Figures 11, 12, 13, and 15 were measured about 1 year after the data in Figures 1−10. Note that the relative intensities of the 25 and 65 °C 7+ ion spectra of Figures 11−13 are somewhat higher than those in Figure 7.

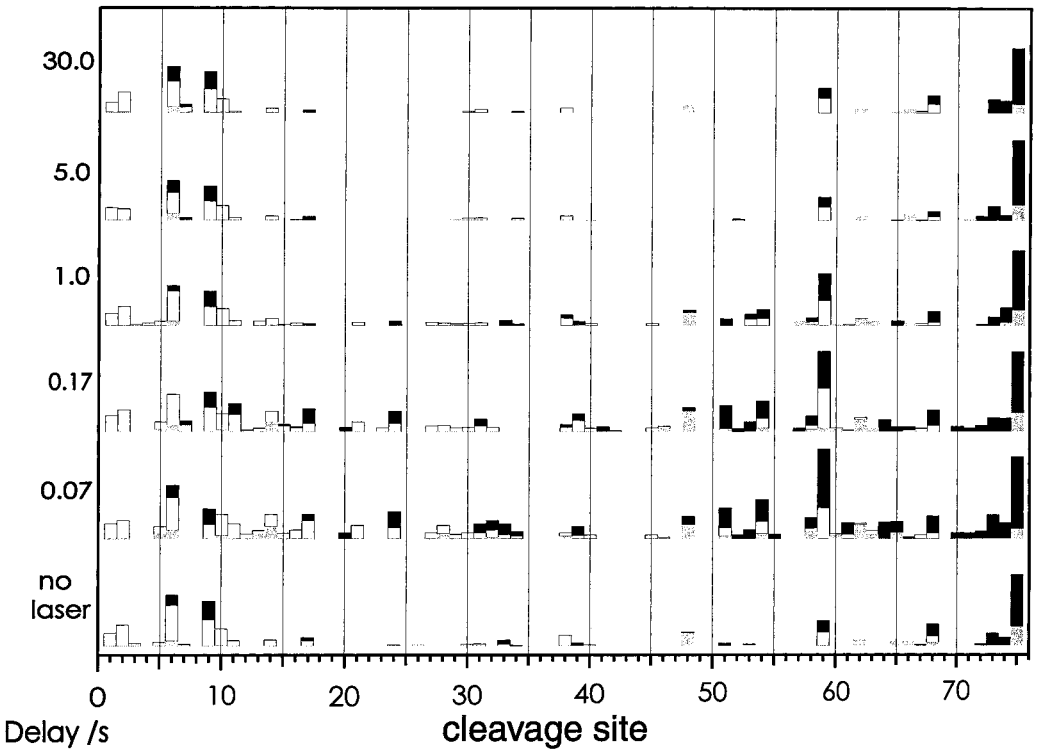

Figure 11. Unfolding/refolding kinetics of ubiquitin 25 °C 7+ ions from ECD spectra. Left column: intervals after pulsed IR laser excitation.

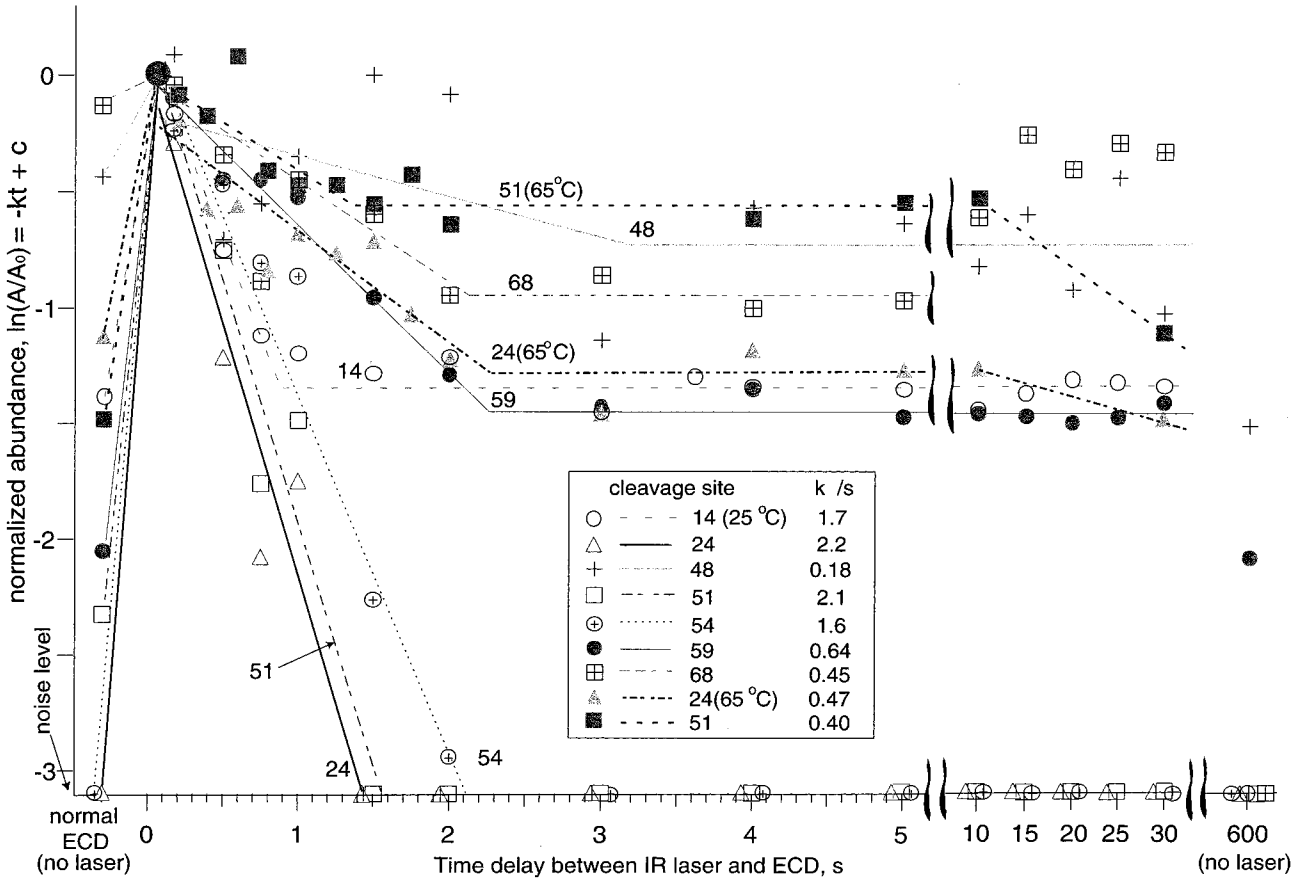

Figure 12. Log of the relative abundances versus time of the ECD peaks from Figure 11 for selected cleavage sites.

Unfolding Involving Specific Backbone Sites. The site-specific normalized intensities of separated ECD dissociation products of the 6+ to 9+ ions at 25−175 °C are shown in Figures 6−9. The number of cleavages between the 75 ubiquitin amino acid pairs increases from none for the 5+ ions at 25 °C to 50 for the 9+ ions at 175 °C. These data provide melting

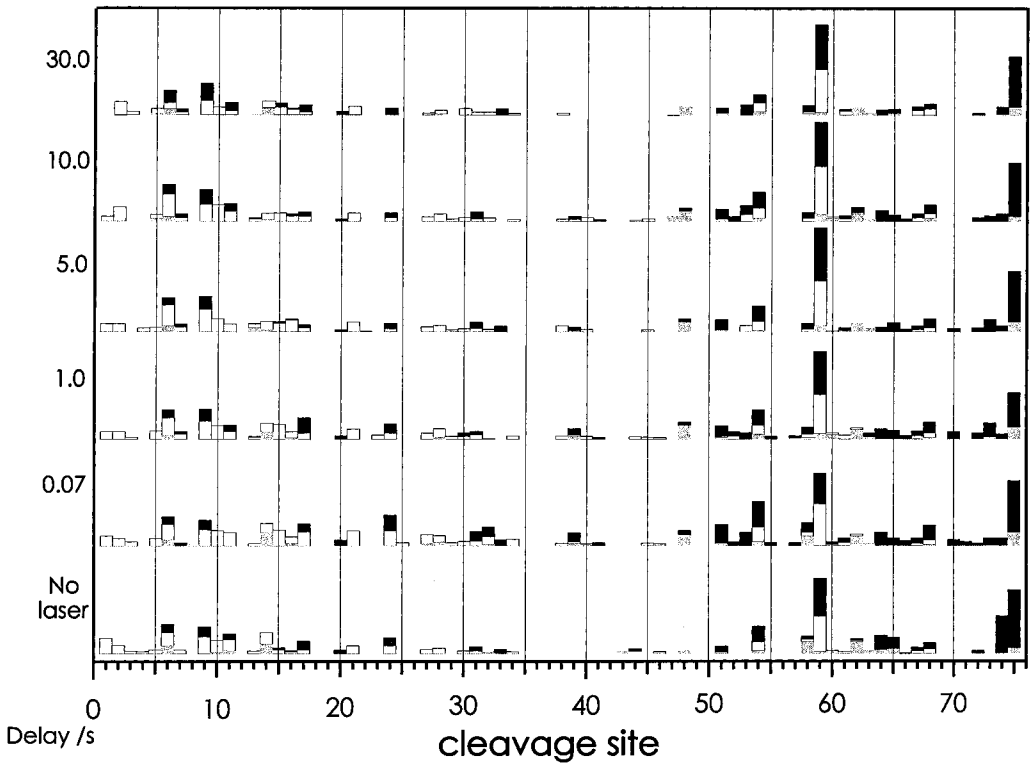

Figure 13. Unfolding/refolding kinetics of ubiquitin 65 °C 7+ ions, as in Figure 11.

temperatures (Figure 14, see Results) for 39 cleavage sites, although these show a substantial range of experimental accuracies. Again, there appears to be no direct relationship between the melting point values for the gaseous ions and those expected for the solution native structure.[6,10,11]

Multiplicity of Conformational Intermediates for Gaseous Ion Unfolding. From the collision cross section data for ubiquitin ions, approximate melting points for C → P of 6+ and 7+ ions are 80 and 50 °C, respectively,[1c,18] while from ECD (Figure 10) these are 156 and 87 °C. The 40 s ion equilibration in the heated ICR cell apparently achieves more complete conformational equilibration (vide infra) than those of the ion mobility and pulsed IR laser experiments. In each charge state many melting point values are sufficiently similar (Figure 14) to suggest that major portions of the backbone undergo cooperative unfolding, as shown in Figure 12 in support of the three-state unfolding mechanism.[1c] However, Figures 6−9 and individual melting point values (Figure 14) show intermediates in the C → P thermal unfolding not shown in Figures 11−13 and only partially indicated in the unfolding caused by increasing charge (Figure 3).

At room temperature the 6+ ions are unfolded only near their termini (Figure 6), mainly up to bond 10 and down to 74. By 115 °C, bonds 11−17 and 73−59 are opening, with bonds up to 31 and down to 51 not inhibited at highest temperatures. In the 7+ ions (Figure 7), however, the melting point for bond 38 cleavage drops dramatically, even below the cleavages in the 21−33 and 51−58 regions. Again, specific stable intermediates are indicated with increasing temperature, but these are structurally distinct from those of the C → P unfolding of the 6+ ions. The lack of central cleavage (bond 38, etc.) for 6+ ions even at higher temperatures cannot be due to the lack of a protonated site; the Figure 3 data indicate that there must be three protons in this region, so that it is the strong noncovalent bonding that prevents separation of any ECD product ions from 6+ ion cleavage. For the 7+ ions, one more proton in the center appears to cause the dramatic decrease in the melting point (Figure 14) of noncovalent bonding around the central bond 38; this could be due to the increase of intramolecular electrostatic repulsion or more favorable solvation of the protonated Arg42 chain to provide the ECD reaction intermediate.[27]

In similar fashion, the addition of another proton forming the 8+ ions then destabilizes the noncovalent bonding in the 21−33 and 51−58 regions (Figure 8). Although the ΔH(unfolding) data (Figure 10) indicate that heating the 8+ ions mainly causes the P → U conformer transition,[18] their ECD spectra (Figure 8) indicate further stable intermediates not obvious in the P → U unfolding of the 7+ ions at >105 °C. For example, the 105−125 °C 7+ ECD spectra are much more similar to each other than to the 75−95 °C 8+ spectra, despite their comparable K(unfolding) values (Figure 10). Similarly, the low-temperature spectra of the 9+ ions (Figure 9) indicate further stable intermediates.

Although adding thermal energy activates all parts of the ubiquitin ion, adding a proton activates selectively the region (or regions) of increased H^+ density. This is in contrast to solution, where increasing the proton concentration (i.e., acidity) instead affects the medium that surrounds the native conformational structure, with protonation of the side chains solvated in the aqueous phase, and with the Coulombic repulsion of these charge sites further shielded by the high dielectric constant of water and offset by deprotonation at acidic residues.

(27) Subjecting the ECD-reduced 7+ ions, $(M + 7H)^{6+\bullet}$, to CAD[4c] or IRMPD gave spectra (not shown) mainly of $\boldsymbol{c}$, $\boldsymbol{z}^{\bullet}$ ions that represent far more significant cleavages at bonds 21, 24, 51, and 59 than those at 38, 39, 48, and near the termini. Initial e^- capture at the latter bonds produced more dissociated products, as shown in the ECD spectrum of the 7+ ions (Figure 7), so that fewer of the undissociated $(M + 7H)^{6+\bullet}$ ions had these bonds cleaved.

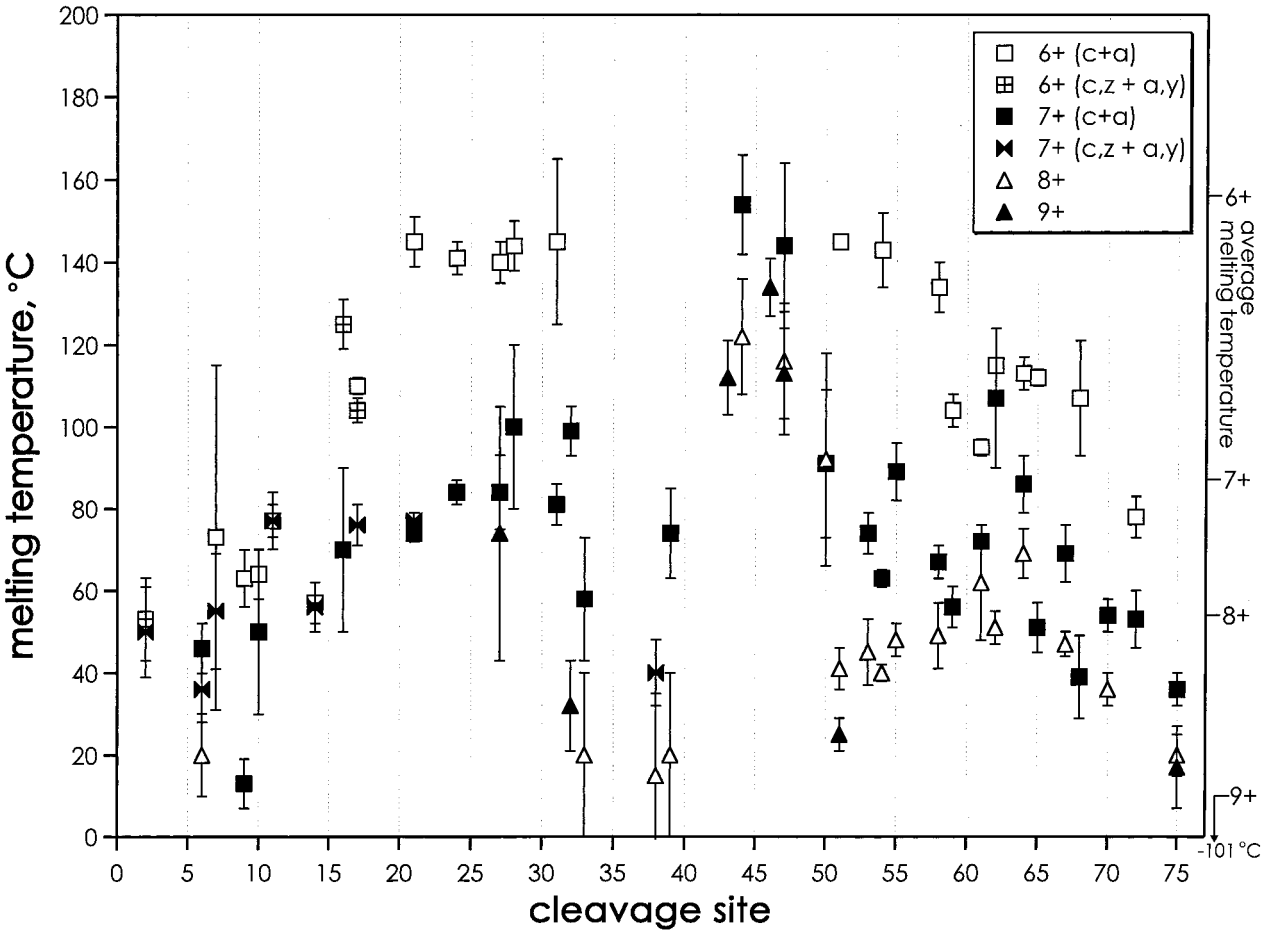

Figure 14. Melting temperatures for 6+ to 9+ ions versus cleavage site. Right axis: overall melting temperatures from Figure 10.

Higher Stability Conformers. In cytochrome *c* 15+ ions, folding continued for several minutes during ion storage under collision-free conditions in the FTICR cell.[3] For the gaseous 7+ ubiquitin ions, some ECD cleavages show a slow folding component (Figure 12); the resulting increased stability has no apparent effect on their rate of unfolding, as pulsed laser excitation after 2 min ion storage gave nearly the same 0.07 s ECD spectrum as that in Figure 11. However, for the far more denatured 9+ ions, after 10 min storage under collision-free conditions at 25 °C the ECD spectra show (Figure 15, top) significant "conformational cooling", with the region of bonds 20−40 now resembling that of the 7+ ions. Further, these 10 min delay spectra are poorly reproducible; Figure 15 (bottom) shows the two most variant of the seven measured to yield the average 10 min spectrum. Here the ECD spectra should be sensitive to the effect of the tertiary noncovalent bonding on both the separation of $c,z^{\bullet}$ products and the solvation of a central protonated side chain to carbonyl groups closer to the termini.[27] This is further evidence of the structural disparity of the solution and gaseous conformers, even though the 10 min equilibration may not yet have allowed formation of the most stable gaseous conformers.

Helical Ion Structures? The A state of ubiquitin, which is largely α-helical, is formed in less polar solvents.[6e,f] In vacuo, an α-helical structure is indicated for Ac-Ala$_n$-LysH$^+$ peptides, stabilized by hydrogen bonding of the charged C-terminal Lys with adjacent carbonyl groups and interaction of the charge with the helix dipole.[22] Such an interaction is consistent with the 13+ ion (Figure 5) cleavages involving a protonated site on the C-terminal side. For the ECD spectra in Figures 6−9, and even Figure 15, the number of amino acids between the major cleavages is surprisingly consistent, with most corresponding to intervals of 3 or 4 residues; the repeat of an α-helix is 3.7 residues. Thus denaturing of the tertiary noncovalent gaseous structure could leave an α-helix that is additionally stabilized by backbone solvation of its protonated side chains.

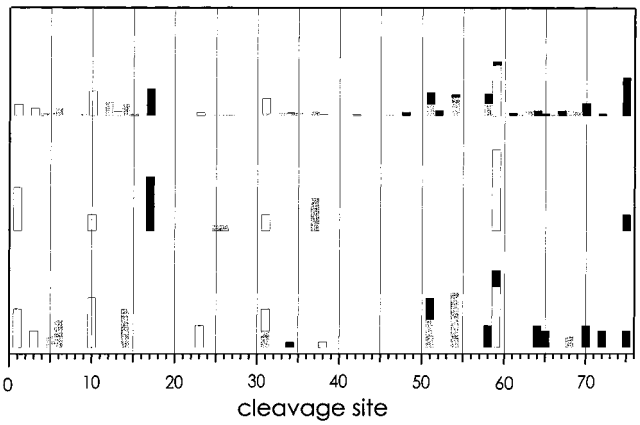

Figure 15. ECD spectra of 25 °C 9+ ions after storage for 10 min in the FTICR cell. Top: average of 7 such individual spectra. Bottom: the two spectra most different from the average.

Conclusions

ECD has provided information on melting points of the tertiary noncovalent bonding at over half of the 75 interresidue sites of the gaseous ubiquitin ions as a function of both charge state and temperature, and in all but 6 sites in some charge/temperature combinations. There is no evidence for the high ΔH(unfolding) value of the 23−34 α-helix and 1−17 β-hairpin found in solution,[6a] consistent with a substantial reduction in hydrophobic bonding in the gas phase.[2d,3] The three-state unfolding C → P → U indicated by the ions' collision cross section data[1] is consistent with overall ΔH(unfolding) values and with similar melting temperatures and refolding kinetics that indicate cooperative unfolding at many sites. Although heating 6+ ubiquitin ions to 175 °C only causes C → P unfolding, the alternative denaturation effected by adding five protons completely destroys the tertiary noncovalent bonding. In addition, this protonation stabilizes the resulting secondary structure (possibly an α-helix) through backbone solvation of the newly protonated side chains, leading to a near-linear[1h] structure with strong secondary interactions at high charge values; in solution these side chains instead would be externally solvated, leading to complete denaturation at high acidity. As also found for gaseous cytochrome *c* ions,[3] it appears unreasonable to expect any close structural relationship between the native conformer of any protein and its gaseous counterparts. This also raises serious questions concerning the characterization of solution intermolecular noncovalent complexes based on their gas-phase behavior.[7] Although a close gas−solution resemblance has been demonstrated for the glycopeptide vancomycin in a strongly hydrogen bonded complex,[7c] any hydrophobic bonding important to a protein complex will be substantially reduced on transfer to the gas phase.

ECD finds that each of the C, P, and U states represents many individual conformers of generally similar tertiary noncovalent structures of closely comparable energies. Further, for each charge state, isomers are possible that represent the protons located at different basic residues. The addition of a proton gives a localized increase in electrostatic repulsion, making the formation of other individual tertiary conformers competitive, as well as adding secondary structure by proton solvation. This unfolding that is generally consistent with a three-state scheme, but which involves a remarkable variety of intermediates and related reactions pathways, recalls the "folding funnel" view in which diverse noncovalent associations lead to ensembles of individual chain conformations that can fold in parallel reaction paths.[5c−f] The poor reproducibility of the 9+ ion spectra after a 10 min equilibration (Figure 15) appears to be due to the huge statistical variation predicted for folding pathways not designed by natural selection, as well as a much smaller enthalpic driving force. The multiplicity of pathways to conformational equilibrium is reminiscent of the problem proposed in "Levinthal's Paradox".[28]

Acknowledgment. We thank Barry Carpenter, Aaron Frank, Ying Ge, Harold Scheraga, and Newman Sze for helpful discussions, and the National Institutes of Health (Grant No. GM16609) for generous funding.

JA012267J

(28) Levinthal, C. *J. Chim. Phys.* **1968**, *65*, 44−45.